

Supporting Information

Lunardi et al. 10.1073/pnas.1002447107

SI Methods

IVEC Procedure. Production and purification of MBP-Dmp53. The ORF of *Drosophila* p53 (NM_206545) was cloned in a modified version of the pFastBac baculovirus expression vector, in frame with maltose binding protein (MBP) at the N terminus (pFB6-MBP-Dmp53). Baculovirus expressing MBP-Dmp53 (or MBP alone as a control) was prepared and used for protein production in Sf9 insect cells. MBP proteins were purified from baculovirus-infected Sf9 cells using amylose beads under nondenaturing conditions [lysis buffer: 20 mM Tris-HCl (pH 7.5), 200 mM NaCl, 1 mM EDTA (pH 8), 10 mM beta-mercaptoethanol]; after extensive washes, beads were used for in vitro pull-down experiments. We observed that best results were obtained using fresh preparations of MBP-Dmp53 and MBP proteins, so each round of pull-down experiments was performed with a different batch of recombinant proteins.

Preparation of small pools. We prepared pools of 24 clones corresponding to single rows of 384-well plates. For the DGC1.0 library, we purified plasmid DNA from mixed bacterial cultures. For the DGC2.0 library, we purified DNA from individual clones using 96-well format minipreps and made pools by mixing plasmid preparations. This procedure required a greater effort in the preparation phase, but greatly facilitated retrieval of positive clones during sib selection.

In vitro pull-down. Radiolabeled proteins were obtained from DNA pools by in vitro transcription–translation in the presence of [³⁵S] methionine, using rabbit reticulocyte lysates (TnT; Promega) and appropriate RNA polymerases. Plates 1–4 of DGC1.0 are cloned in pBluescript vectors and translate with poor efficiency. To overcome this problem, we used primers with vector sequences to amplify the inserts by PCR, the upper primer containing a T7 RNA polymerase promoter for in vitro transcription, exactly as described by others (1).

PCR products were directly used as templates for coupled in vitro transcription–translation. Plates 1–8 of DGC2.0 are cloned in pFLC vectors and do not translate efficiently in reticulocyte lysates. Expression of these clones was not improved by a PCR-based approach, so they had to be excluded from this study.

Radiolabeled proteins were added to small aliquots of recombinant MBP-Dmp53 bound to amylose beads. After a 1 h incubation in pull-down buffer [50 mM Tris-HCl (pH 7.5), 150 mM NaCl, 0.1% Nonidet P-40, 5% glycerol, protease inhibitors (Sigma), 1 mM PMSF, 5 mM NaF, 1 mM beta-glycerolphosphate], the reactions were transferred to plastic minifilters (Wizard Minicolumn; Promega) mounted on a vacuum manifold, and the beads were washed by passing a large volume of pull-down buffer through the column. Bound proteins were eluted with hot Laemmli sample buffer by briefly centrifuging the filters on top of 1.5-mL tubes. Eluted proteins were analyzed by SDS/PAGE followed by autoradiography.

Bioinformatics and Statistical Analysis. Data compilation. The list of literature-curated *Drosophila* p53 interactions (LCDI) includes proteins with at least one experimental evidence of physical interaction with Dmp53 and excludes phenotypic and functional associations. It was compiled by searching a number of protein–protein interaction databases: BioGrid, MINT, DroID, IntAct, BIND, and HPRD. It also contains additional physical interactions involving Dmp53 described in the literature. The data included in the LCDI dataset were last updated on February 27, 2009. Human orthologs were defined according to Homologene and Inparanoid databases (<http://inparanoid.sbc.su.se/>). For genes

lacking a human ortholog in these databases, we performed BLAST analysis vs. human protein sequences and focused our attention on hits with a significant similarity score. We used the BLASTO interface (<http://oxytricha.princeton.edu/BlastO/>) to compare peptide sequences vs. clusters of eukaryotic orthologous groups (NCBI_KOG and MultiParanoid) (2). Finally, we employed TreeFam (<http://www.treefam.org/>) to construct phylogenetic trees of putative ortholog groups. In some cases, humans have more than one gene with significant similarity to a single *Drosophila* gene: if the human genes are phylogenetically related to each other (i.e., paralogs) they were all considered orthologs (e.g., *Drosophila Imp* vs. human IGFBP1, IGFBP2, and IGFBP3). In other cases, *Drosophila* has two or more paralogs with significant similarity to a single human gene (e.g., *Drosophila eyeless* and *twi-of-eyeless* vs. human Pax6): In such instances, the human gene was considered an ortholog to both. In some cases we detected strong similarity only within a specific domain of the protein, with poor conservation along the remaining peptide sequence. In those instances, we considered them orthologs only if the two proteins scored as reciprocal best matches in BLAST analysis.

Overrepresentation analysis. Overrepresentation analysis of Gene Ontology and phenotypes among the interactors was performed using Fisher's exact test. The background populations are the lists of all fly genes represented in the DGC 1.0 and 2.0 libraries (6,607 FlyBase IDs). Gene Ontology and phenotype annotations were obtained from FlyBase. For both Gene Ontology and phenotype annotation we took into account the hierarchical nature of the annotation ontologies by assigning to each gene all of the annotation terms that are ancestors in the ontology of the terms that are directly assigned to the gene. To avoid very generic GO terms the analysis was limited to terms with a total prevalence <2,000 in the background population.

Relevance to cancer. We analyzed publicly available breast cancer gene expression datasets to determine which of the functionally validated human interactors have prognostic predictive power. The datasets analyzed are as follows:

NKI: Described in ref. 3. Normalized expression data and clinical data were obtained from the paper's website (<http://www.rii.com/publications/2002/nejm.html>).

Miller (4): Normalized expression data and clinical data were obtained from the Gene Expression Omnibus (GEO) website (<http://www.ncbi.nlm.nih.gov/projects/geo/>) under accession GSE3494.

Pawitan (5): Normalized expression data and clinical data were obtained from GEO under accession GSE1456.

We considered only probesets associated unambiguously with one of the functionally validated human interactors by the annotation file provided by Affymetrix. For the NKI datasets, the mapping between accession numbers provided in the original dataset and Entrez Gene IDs was obtained through Unigene. We used univariate Cox analysis to determine significant ($P \leq 0.05$) correlations between the logarithmic expression of each microarray probeset and patient survival. For GTPBP4 in p53-wild-type breast tumors we also compared the survival probabilities of high- and low-GTPBP4 tumors with a log-rank test. For this analysis the logarithmic expression levels of the two Affymetrix probes associated with GTPBP4 were averaged.

Databases. Databases used were as follows: FlyBase release 2008_05; BioGrid release 2.0.45; DroID version 4.0; Homologene version 62, released June 12, 2008; Inparanoid version 6.0, released August

2007; NCBI_KOG release 2003; MultiParanoid release 2006; TreeFam version 6.0, released June 6, 2008; Entrez Gene, downloaded 26 October 2008; Gene Ontology release 20081012; Affymetrix HGU133 annotations, version 26; and Unigene, *Homo sapiens* build 216.

Cell Culture and Transfection Methods. SF9 insect cells were cultured at 27 °C in SF900II medium (Gibco) supplemented with 10% FBS and gentamycin (10 µg/mL). HEK293T, HCT116, and U2OS mammalian cell lines were cultured in Dulbecco's modified Eagle's medium supplemented with 10% FBS, penicillin (100 units/mL), and streptomycin (100 µg/mL). Calcium phosphate was used for DNA transfection of HEK293T and U2OS. siRNAs were transfected using RNAiMAX and Lipofectamine 2000 reagent (Invitrogen).

Quantification of Cell Viability Using WST-1. Cell viability was assayed using the WST-1 reagent (Roche), according to the manufacturer's protocol. Absorbance was measured on a microplate ELISA reader (Envision Xcite; Perkin-Elmer) at a 450-nm detection wavelength. Normalized WST was calculated as follows: WST (%) = [(A₄₅₀ of treated sample - A₄₅₀ of blank)/(A₄₅₀ of untreated sample - A₄₅₀ of blank)] × 100. Blank represents wells containing culture medium only.

For any given siRNA pool, the difference in normalized WST between untreated and drug-treated cells [Δ WST = WST(untreated) - WST(treated)] reflects the amplitude of the effect of p53 activation. Δ WST values of cells transfected with interactor-specific siRNAs were compared to Δ WST values of cells transfected with control siRNAs (two independent nontargeting siRNAs were used as controls). A greater Δ WST indicates more efficient arrest, and a smaller Δ WST indicates less efficient arrest. Differences were considered significant if they were >10 normalized WST units [i.e., Δ WST(interactor siRNA) - Δ WST(control siRNA) > |10|].

Real-Time RT-PCR. Total RNA was isolated using the TRIZOL reagent (Invitrogen), following the manufacturer's instructions. Single-strand cDNA was obtained from 1 µg of purified RNA, using the iSCRIPT cDNA Synthesis Kit (Bio-Rad) according to manufacturer's instructions. Quantitative RT-PCR (qPCR) was performed using SYBR-Green PCR Master Mix (Applied Biosystems) and an iCycler IQ Real-time PCR System (Bio-Rad). Expression of the gene of interest was analyzed using specific oligonucleotides designed using the software Beacon Designer 2.0 (Premier Biosoft International). Primer sequences are available upon request. The annealing temperature of all of the primers described was 60 °C. The results were normalized to GAPDH and the initial amount of the template of each sample was determined as relative expression vs. that of one of the samples chosen as reference. The relative expression of each sample was calculated by the equation $2^{-\Delta\Delta C_t}$ (User Bulletin 2 of the ABI Prism 7700 Sequence Detection System).

Protein Interaction Studies. Expression vectors encoding MBP-fusion proteins. For coaffinity purification assays, the MBP coding sequence from pMalC2x was PCR amplified and cloned in pcDNA3.1 expression vector, with a Kozak consensus for efficient translation in mammalian cells. The coding regions of human p53, Tap63alpha, and Tap73alpha were inserted in frame at the C terminus of MBP to generate the pcDNA3-MBP-p53, pcDNA3-MBP-p63, and pcDNA3-MBP-p73 plasmids.

Coimmunoprecipitation. Co-IP experiments with endogenous proteins were performed in HCT116 cell lines using co-AP buffer [50 mM Tris-HCl (pH 8), 150 mM NaCl, 1 mM EDTA (pH 8), 1 mM DTT, 5% glycerol, protease inhibitors (Sigma), 1 mM PMSF, 5 mM NaF, 1 mM beta-glycerolphosphate]. Samples were cleared by centrifugation for 30 min at 13,000 × g at 4 °C and incubated for 2 h at 4 °C with anti-p53 antibody (DO-1; Santa Cruz). After 1 h incubation with protein G-Sepharose (GE Healthcare), immunoprecipitates were washed three times in co-AP buffer, resuspended in sample buffer, and analyzed by immunoblotting. To avoid cross-reaction with Ig heavy chains, immunoprecipitated p53 was detected using rabbit polyclonal FL393 (Santa Cruz) followed by HRP-Protein A (Pierce). For Co-IP of overexpressed proteins, p53-null H1299 cells were transfected with appropriate expression vectors and processed 48 h later. Lysis was performed in co-AP buffer supplemented with phosphatase and protease inhibitors. Cleared lysates were incubated overnight with anti-GFP or anti-HA antibody covalently bound to Protein G-Sepharose (GE Healthcare), using 10 mg/mL dimethylpimelidate (Pierce). Immunoprecipitated proteins were separated by SDS/PAGE and analyzed by immunoblotting. Coimmunoprecipitated p53 was directly detected using HRP-conjugated DO-1 monoclonal antibody (Santa Cruz).

In vitro pull-down using purified proteins. The MBP and MBP-p53 baits were purified from H1299 cells transfected with the respective pcDNA3 expression vectors. Cells were lysed in co-AP buffer and MBP-fusion proteins were recovered on amylose beads (NEB).

For expression in bacteria, the coding region of human GTPBP4 was cloned in frame at the C terminus of GST in pGEX4T1. Recombinant GST and GST-GTPBP4 proteins were purified from BL21 after induction with 1 mM IPTG for 2 h at 37 °C. Bacteria were lysed in 50 mM Tris-HCl (pH 8.0), 300 mM NaCl, 0.1% Nonidet P-40, 0.1% Triton X-100, 0.1% Tween 20, 1 mM EDTA, plus 0.2 mg/mL lysozyme and protease inhibitors. After 30 min on ice, lysates were sonicated, clarified by centrifugation, and incubated with glutathione beads (GE Healthcare). After purification, GST and GST-GTPBP4 proteins were eluted with 10 mM reduced glutathione and used as prey for in vitro pull-down on MBP and MBP-p53 beads. After 1 h binding at 4 °C in co-AP buffer, beads were washed and bound proteins were analyzed by Western blot.

- Lee LA, et al. (2005) *Drosophila* genome-scale screen for PAN GU kinase substrates identifies Mat98Bb as a cell cycle regulator. *Dev Cell* 8:435-442.
- Zhou Y, Landweber LF (2007) BLASTO: A tool for searching orthologous groups. *Nucleic Acids Res* 35:W678-W682.
- van de Vijver MJ, et al. (2002) A gene-expression signature as a predictor of survival in breast cancer. *N Engl J Med* 347:1999-2009.

- Miller LD, et al. (2005) An expression signature for p53 status in human breast cancer predicts mutation status, transcriptional effects, and patient survival. *Proc Natl Acad Sci USA* 102:13550-13555.
- Pawitan Y, et al. (2005) Gene expression profiling spares early breast cancer patients from adjuvant therapy: Derived and validated in two population-based cohorts. *Breast Cancer Res* 7:R953-R964.

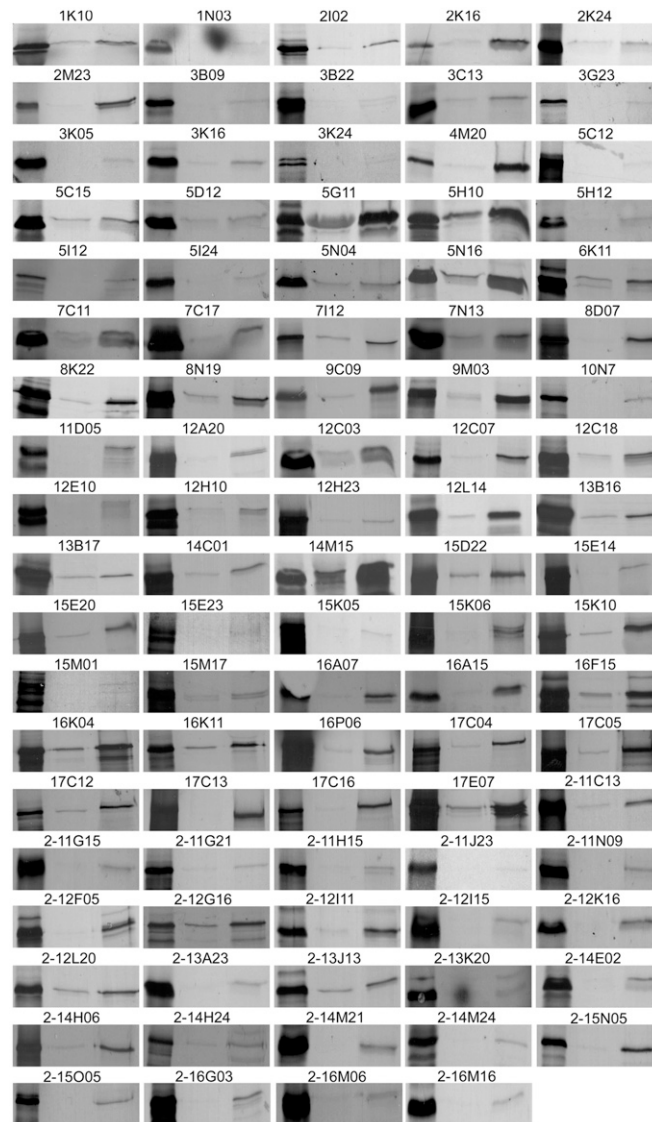


Fig. S1. In vitro pull-down experiments relative to the 94 cDNA hits identified during the screening. Each first lane is 1/40th of the input. Each second lane is the eluate of MBP beads. Each third lane is the eluate of MBP-Dmp53 beads. Numbers represent the position of each clone in 384-well plates of the DGC1.0 and DGC2.0 libraries. Clone 12L14 is Dmp53 (FBgn0039044). Clone 17E07 (LD46618P) is not annotated in FlyBase and corresponds to a "probable RNA-directed DNA polymerase from transposon BS." Identity of the *Drosophila* genes corresponding to all remaining clones can be found in [Table S1](#).

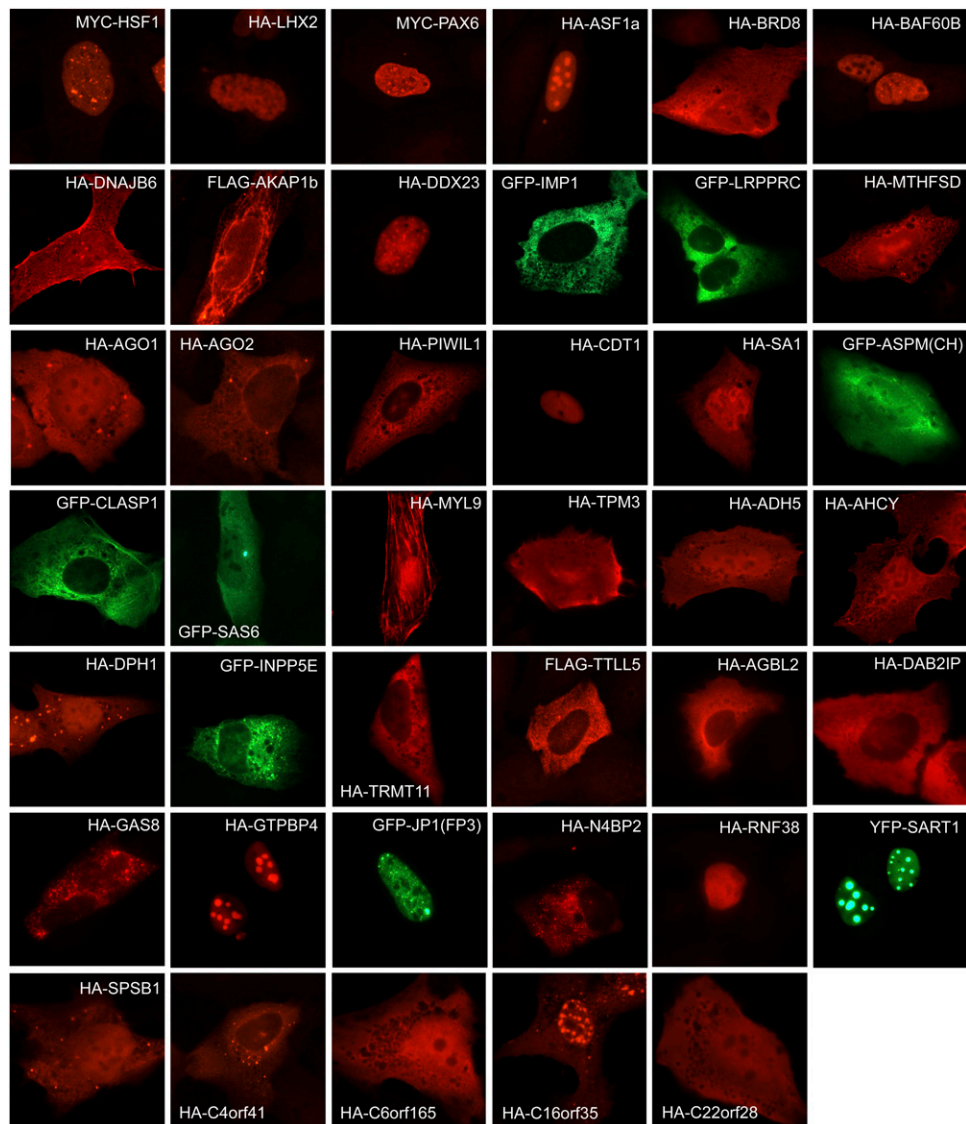


Fig. S2. Cellular localization of 41 mammalian orthologs of Dmp53 interacting proteins. Vectors expressing the indicated proteins were transiently transfected in U2OS cells. Localization of encoded proteins was analyzed by immunofluorescence after 24 h. Proteins were visualized using antibodies to specific epitope tags or by GFP as indicated.

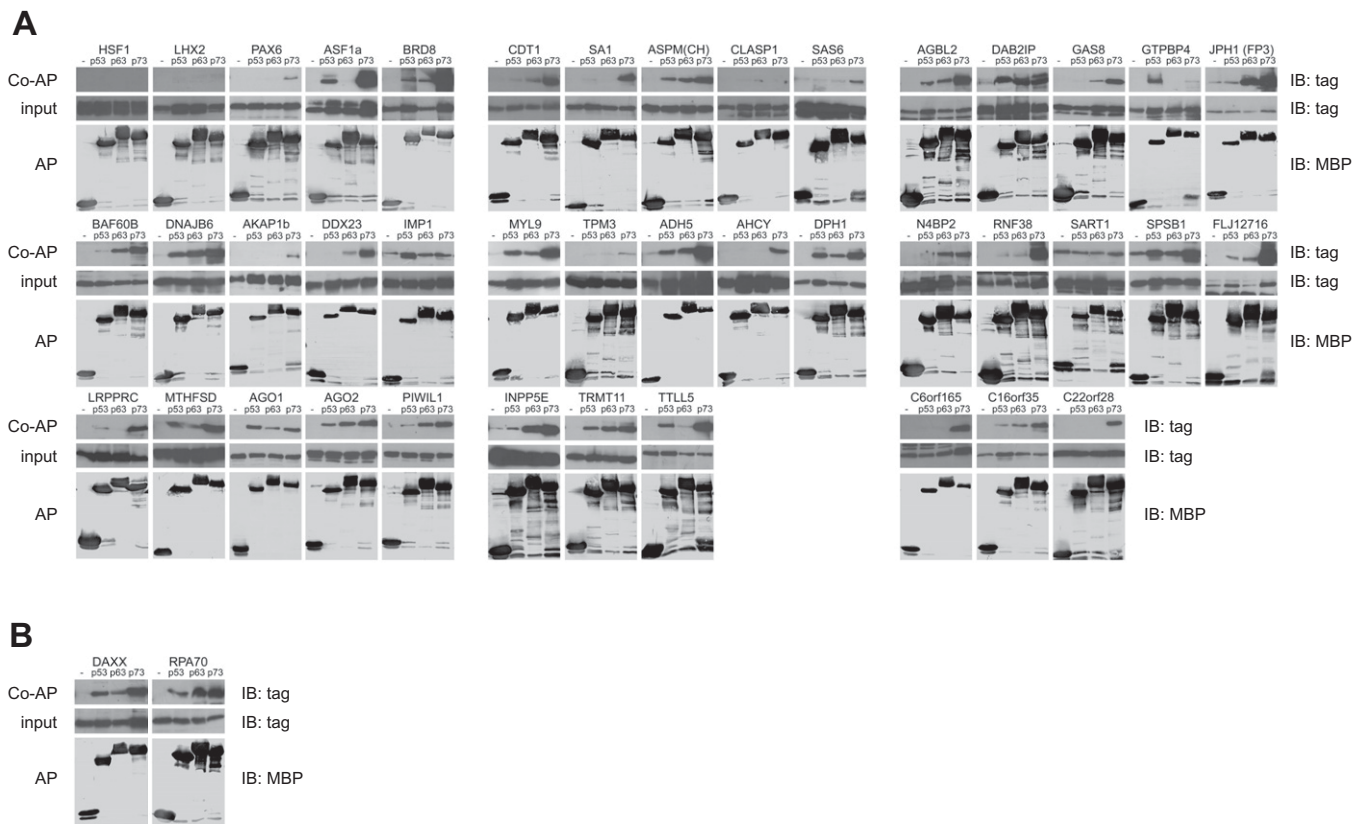


Fig. S3. Co-AP experiments relative to mammalian orthologs of Dmp53 interacting proteins. (A) Expression plasmids encoding tagged versions of the indicated proteins were cotransfected with pcDNA3-MBP, pcDNA3-MBP-p53, pcDNA3-MBP-TAp63a, or pcDNA3-MBP-TAp73a in 293T cells. After cell lysis, MBP fusion proteins (baits) were purified on amylose beads. Copurified proteins were detected by immunoblotting using antibodies to specific tags. (Top) Tagged prey proteins after affinity purification, demonstrating binding to the indicated MBP-tagged bait proteins or MBP alone as a control (-). (Middle) Expression of the tagged prey in the lysate (1/40th of the input). (Bottom) Expression of MBP-tagged bait proteins after affinity purification. Top and Middle are cropped from the same autoradiographic film (i.e., have the same exposure). (B) As proof of concept for sensibility and reliability of the assay, co-AP experiments using two human p53 interologs (Daxx and Rpa70) are also shown.

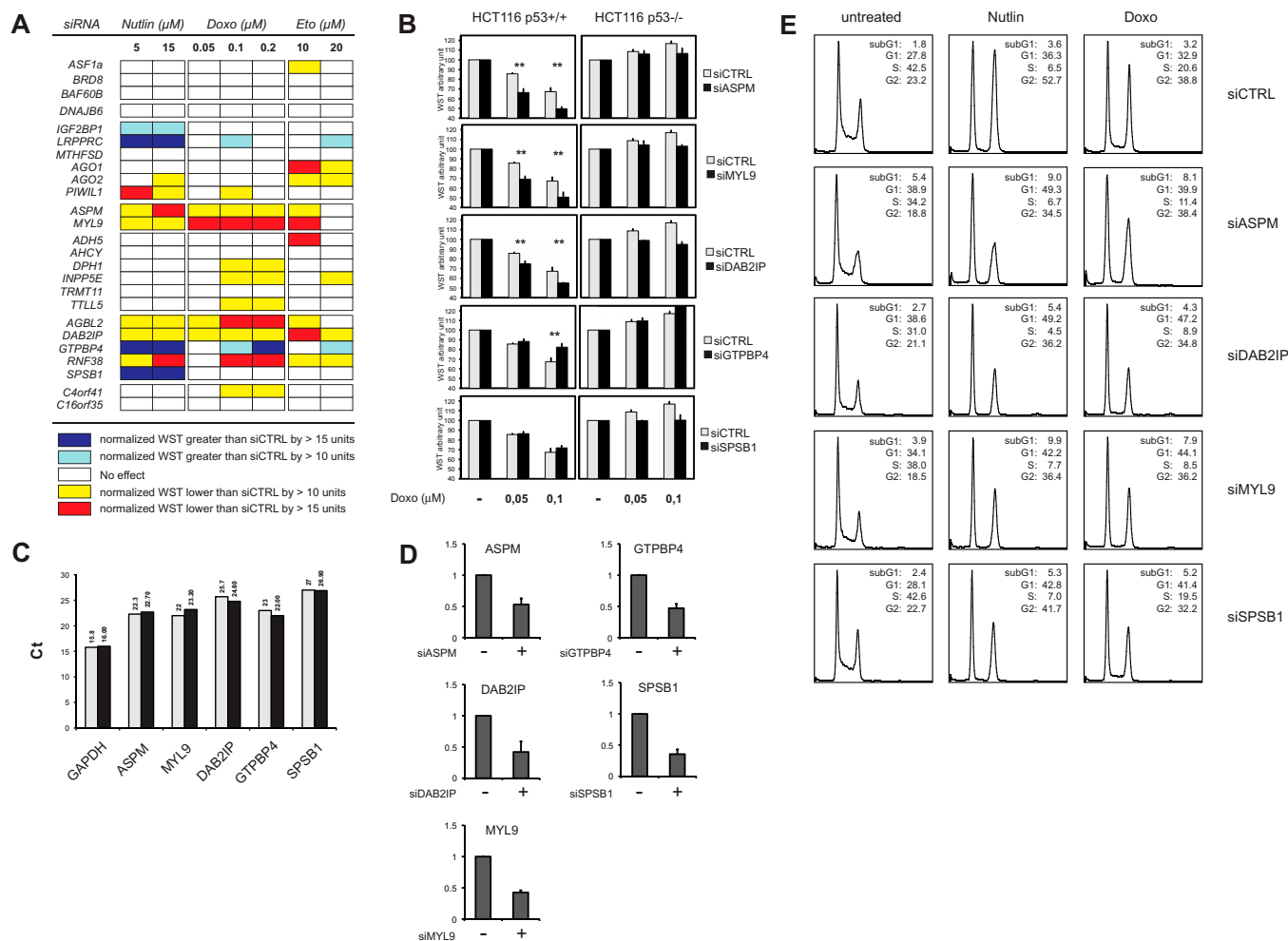


Fig. S4. Functional validation of p53 interactors by RNA-mediated interference. (A) Primary screening for modulators of p53-dependent growth inhibition. HCT116 cells bearing wild-type p53 (HCT116 WT) were transfected with control siRNA (siCTRL) or siRNA pools targeting each of 24 newly identified p53 interactants. Cell viability was measured by WST-1 after treatment with Nutlin-3, Doxorubicin, or Etoposide as indicated. The difference in normalized WST between untreated and treated samples (Δ WST) was used to quantify the decrease in cell viability after p53 activation. For each gene-specific siRNA, this value was compared to that of control siRNA; differences in Δ WST were considered significant only if reproducibly >10 normalized WST units (see *SI Methods* for details). (B) Transient knockdown of five unique p53 interactors affects the response of HCT116 cells to Doxorubicin. The experiment was performed as described in Fig. 3A. As a control for p53 dependency, the same experiment was performed in HCT116 p53^{-/-} cells (*, $P < 0.05$; **, $P < 0.01$). (C) Functionally validated p53 interactors are expressed at comparable levels in HCT116 WT cells (gray bars) and HCT116 p53^{-/-} cells (black bars). mRNA levels of the indicated genes were analyzed by RT-qPCR. A single representative experiment is reported. (D) All siRNA pools reduce the levels of target mRNAs to $\leq 50\%$. Expression levels of the five functionally validated p53 interactors were determined by RT-qPCR in HCT116 WT cells transfected with control or specific siRNA pools under the experimental conditions used for WST assays. Data are averages \pm SD. (E) Cell-cycle analysis of cells transiently transfected with siRNA pools targeting four different functional hits. HCT116 p53 WT cells were lipofected with the indicated siRNA pools, treated with Nutlin-3 (5 mM) or Doxorubicin (0.05 mM) for 24 h, stained with propidium iodide (PI), and analyzed by flow cytometry. The distribution (percentage) of cell-cycle phases was determined using FlowJo software.

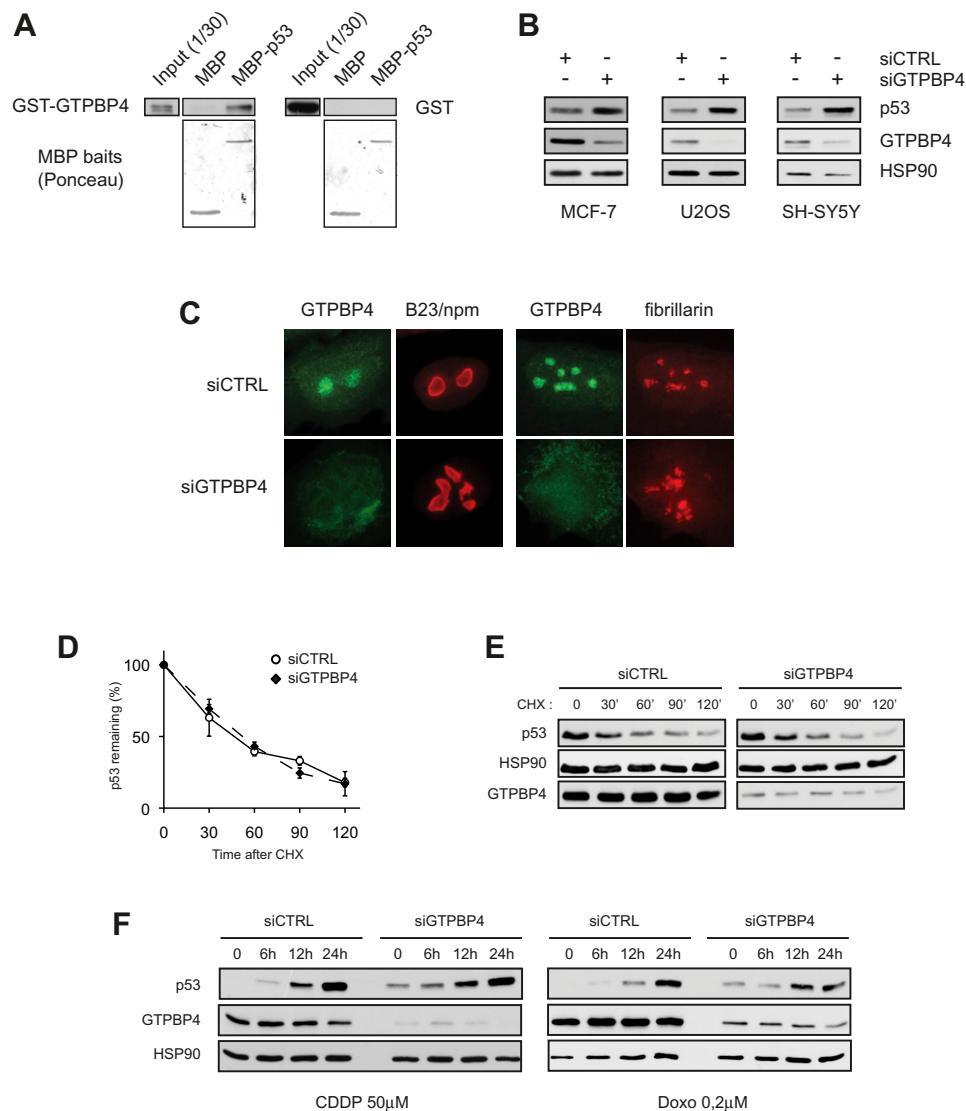


Fig. S5. Additional evidence of physical and functional interaction between GTPBP4 and p53. (A) Purified GTPBP4 and p53 interact in vitro. Recombinant GST and GST-GTPBP4 proteins were expressed in bacteria, purified on glutathione-Sepharose beads, eluted, and used for in vitro pull-down assays on amylose beads loaded with MBP or MBP-p53 purified from transfected H1299 cells (*SI Methods*). GST-GTPBP4 is produced with poor efficiency in bacteria, so the protein was detected by immunoblotting. (Upper) GST-GTPBP4 (Left) or GST (Right) proteins copurified with MBP or MBP-p53 beads, compared to 1/30th of the input. (Lower) Affinity-purified MBP baits. (B) Knockdown of GTPBP4 induces accumulation of p53 in multiple cell lines. p53 expression was analyzed by immunoblotting of the indicated human transformed cells after transfection of control or GTPBP4 siRNA. A specific antibody to GTPBP4 confirmed efficient knockdown of the endogenous protein. Hsp90 was detected in the same lysates as a loading control. (C) GTPBP4 knockdown does not affect localization of key nucleolar proteins. Immunofluorescence analysis is shown of GTPBP4, B23/nucleophosmin, and fibrillarlin in U2OS cells transfected for 48 h with either control or GTPBP4 siRNA. Nuclei are counterstained with Hoechst. (D) GTPBP4 knockdown does not induce p53 stabilization. Quantification is shown of the ratio of p53 to Hsp90 (measured by densitometry on Western blots) in HCT116 WT cells transfected with GTPBP4 siRNA (solid diamonds) or control siRNA (open circles) for 48 h and treated for the indicated times with 50 μ M Cycloheximide (CHX). Data are means \pm SD for three independent experiments. (E) Representative Western blot used for the analysis of p53 half-life. To obtain a comparable p53 signal, the gel was loaded with 15 μ g lysate of control siRNA samples (Left), and 7.5 μ g lysate of GTPBP4 knockdown samples (Right). Immunoblotting for GTPBP4 confirmed efficient knockdown of the endogenous protein. (F) Depletion of GTPBP4 does not impair p53 accumulation in response to DNA damage. HCT116 WT cells were transfected with GTPBP4 siRNA or control siRNA for 48 h and treated for the indicated times with Cisplatin (CDDP) or Doxorubicin. The same amount of total lysate was loaded in all lanes. Blotting for GTPBP4 confirmed efficient knockdown of the endogenous protein. Hsp90 was detected in the same lysates as a loading control.

Table S1. List of Dmp53 interactors identified in the screening (IVDI)

DGC clone	FlyBase ID	Gene	Name
01K10	FBgn0003514	CG3595	SPAGHETTI SQUASH
01N03	FBgn0038876	CG5919	CG5919
02I02	FBgn0025463	CG4303	BRAHMA ASSOCIATED PROTEIN 60KD
02K16	FBgn0034091	CG8448	MRJ
02K24	FBgn0036194	CG11652	CG11652
02M23	FBgn0010173	CG9633	REPLICATION PROTEIN A 70 (*)
03B09	FBgn0014455	CG11654	ADENOSYLHOMOCYSTEINASE AT 13
03B22	FBgn0013773	CG10240	CYP6A22
03C13	FBgn0037814	CG6325	CG6325
03G23	FBgn0087035	CG7439	ARGONAUTE 2 (partial)
03K05	FBgn0011768	CG6598	FORMALDEHYDE DEHYDROGENASE
03K16	FBgn0045063	CG8824	FUSED LOBES
03K24	FBgn0032690	CG10333	CG10333 (partial)
04M20	FBgn0000099	CG8376	APTEROUS
05C12	FBgn0027532	CG7139	CG7139
05C15	FBgn0021944	CG3433	COPROPORPHYRINOGEN OXIDASE
05D12	FBgn0035600	CG4769	CG4769
05G11	FBgn0028530	CG18124	MITOCHONDRIAL TRANSCRIPTION TERMINATION FACTOR
05H10	FBgn0023519	CG3109	MITOCHONDRIAL RIBOSOMAL PROTEIN L16
05H12	FBgn0038487	CG4060	TWEEDLEW
05I12	FBgn0000146	CG6137	AUBERGINE
05I24	FBgn0028473	CG8801	CG8801
05N04	FBgn0016041	CG12157	TRANSLOCASE OF OUTER MEMBRANE 40
05N16	FBgn0029969	CG10932	CG10932
06K11	FBgn0038194	CG3050	CYP6D5
07C11	FBgn0037544	CG11035	CG11035
07C17	FBgn0029094	CG9383	ANTI-SILENCING FACTOR 1
07I12	FBgn0033438	CG1794	MATRIX METALLOPROTEINASE 2
07N13	FBgn0010340	CG9852	UPSTREAM OF RPII140
08D07	FBgn0001133	CG33133	GRAUZONE
08K22	FBgn0038546	CG7379	CG7379 (*)
08N19	FBgn0033235	CG8728	CG8728
09C09	FBgn0019650	CG11186	TWIN OF EYELESS
09M03	FBgn0031191	CG14617	CG14617
10N07	FBgn0037245	CG14648	GROWL
11D05	FBgn0000351	CG11330	CORTEX
12A20	FBgn0001222	CG5748	HEAT-SHOCK FACTOR
12C03	FBgn0066365	CG15013	DUSKY-LIKE (partial)
12C07	FBgn0035852	CG7387	CG7387
12C18	FBgn0037250	CG1074	CG1074
12E10	FBgn0050059	CG30059	CG30059
12H10	FBgn0033367	CG8193	CG8193
12H23	FBgn0039654	CG14514	BRD8
13B16	FBgn0038860	CG10825	CG10825
13B17	FBgn0036397	CG8783	CG8783
14C01	FBgn0038607	CG7669	CG7669
14M15	FBgn0026238	CG2944	GUSTAVUS
15D22	FBgn0052627	CG32627	CG32627
15E14	FBgn0020616	CG3423	STROMALIN
15E20	FBgn0035416	CG17569	GRYZUN
15E23	FBgn0032388	CG6686	CG6686
15K05	FBgn0031820	CG9537	DAXX-LIKE PROTEIN (partial) (*)
15K06	FBgn0000140	CG6875	ABNORMAL SPINDLE (partial)
15K10	FBgn0051108	CG31108	CG31108
15M01	FBgn0052306	CG32306	CG32306
15M17	FBgn0037705	CG9381	MURASHKA
16A07	FBgn0000504	CG11094	DOUBLESEX
16A15	FBgn0003721	CG4898	TROPOMYOSIN 1
16F15	FBgn0024987	CG3056	CG3056
16K04	FBgn0030235	CG1691	IGF-II MRNA-BINDING PROTEIN
16K11	FBgn0029764	CG3249	YU
16P06	FBgn0051738	CG31738	CG31738
17C04	FBgn0032679	CG10302	BICOID STABILITY FACTOR

Table S1. Cont.

DGC clone	FlyBase ID	Gene	Name
17C05	FBgn0259165	CG42270	CG42270
17C12	FBgn0032129	CG4405	JUNCTOPHILIN
17C13	FBgn0002872	CG1960	MUTATOR 2
17C16	FBgn0021760	CG32435	CHROMOSOME BOWS
2_11C13	FBgn0038266	CG3610	CG3610
2_11G15	FBgn0050418	CG30418	NORD (partial)
2_11G21	FBgn0034532	CG13436	CG13436
2_11H15	FBgn0037101	CG7634	CG7634
2_11J23	FBgn0034007	CG8102	CG8102
2_11N09	FBgn0033258	CG8712	CG8712
2_12F05	FBgn0031546	CG8851	CG8851 (partial)
2_12G16	FBgn0029667	CG14271	GROWTH ARREST SPECIFIC PROTEIN 8
2_12I11	FBgn0037454	CG1137	CG1137
2_12I15	FBgn0033953	CG12861	CG12861
2_12K16	FBgn0037626	CG8236	CG8236
2_12L20	FBgn0036731	CG6333	CG6333
2_13A23	FBgn0039124	CG13597	CG13597 (partial)
2_13J13	FBgn0033706	CG13167	CG13167
2_13K20	FBgn0039731	CG15524	SPINDLE ASSEMBLY ABNORMAL
2_14E02	FBgn0029940	CG1958	CG1958
2_14H06	FBgn0033186	CG1602	CG1602
2_14H24	FBgn0000996	CG8171	DOUBLE PARKED
2_14M21	FBgn0050362	CG30362	CG30362
2_14M24	FBgn0001250	CG9623	INFLATED (partial)
2_15N05	FBgn0034037	CG8214	CG8214
2_15O05	FBgn0036273	CG10426	CG10426
2_16G03	FBgn0032781	CG9987	CG9987
2_16M06	FBgn0052985	CG32985	CG32985 (partial)
2_16M16	FBgn0015542	CG7951	SIMILAR (partial)*

*Known Dmp53 interactors and fly orthologs of mammalian proteins already reported to bind p53, p63, or p73 (FlyBase version FB2008_5, released May 30, 2008).

Table S2. List of known Dmp53 interactors (LCDI)

FlyBase ID	Gene	Name	Ref.
FBgn0053554	CG33554	<i>nipped-A</i>	(1)
FBgn0020388	CG4107	<i>Gcn5/PCAF</i>	(1)
FBgn0030891	CG7098	<i>diskette</i>	(1)
FBgn0037555	CG9638	<i>Ada2b</i>	(1)
FBgn0000044	CG10067	<i>Act57B</i>	(2)
FBgn0000166	CG1034	<i>bicoid</i>	(2)
FBgn0010602	CG3018	<i>lesswright*</i>	(2)
FBgn0003479	CG7948	<i>Spindle-A*</i>	(2)
FBgn0023526	CG2865	<i>CG2865</i>	(2)
FBgn0025674	CG15218	<i>CycK</i>	(2)
FBgn0026602	CG1851	<i>Ady43A</i>	(2)
FBgn0030459	CG12723	<i>CG12723</i>	(2)
FBgn0030882	CG6835	<i>GS</i>	(2)
FBgn0031894	CG4496	<i>CG4496</i>	(2)
FBgn0031957	CG14534	<i>TwdlE</i>	(2)
FBgn0028509	CG31811	<i>cenG1A</i>	(2)
FBgn0023091	CG8667	<i>dimmed</i>	(2)
FBgn0035021	CG4622	<i>CG4622</i>	(2)
FBgn0035357	CG1244	<i>CG1244</i>	(2, 3)
FBgn0035397	CG11486	<i>CG11486</i>	(2)
FBgn0035641	CG5568	<i>CG5568</i>	(2)
FBgn0037944	CG6923	<i>CG6923</i>	(2, 3)
FBgn0034410	CG15104*	<i>dTopors*</i>	(3, 4)
FBgn0000633	CG17716	<i>faint sausage</i>	(3)
FBgn0003891	CG9450	<i>tudor</i>	(3)
FBgn0010328	CG5965	<i>woc</i>	(3)
FBgn0011474	CG3307	<i>pr-set7</i>	(3)
FBgn0012049	CG11494	<i>BtbVII</i>	(3)
FBgn0026262	CG2009	<i>bip2/DmTAF3</i>	(3, 5)
FBgn0027499	CG12340	<i>CG12340</i>	(3)
FBgn0027514	CG1024	<i>CG1024</i>	(3)
FBgn0027603	CG12359	<i>Ulp1</i>	(3)
FBgn0031597	CG17612	<i>CG17612</i>	(3)
FBgn0031719	CG18269	<i>CG18269</i>	(3)
FBgn0033636	CG10897	<i>toutatis</i>	(3)
FBgn0034976	CG4049	<i>CG4049</i>	(3)
FBgn0035038	CG13588	<i>CG13588</i>	(3)
FBgn0035047	CG3691	<i>Pof</i>	(3)
FBgn0035849	CG7404	<i>ERR</i>	(3)
FBgn0036668	CG9715	<i>CG9715</i>	(3)
FBgn0037344	CG2926	<i>CG2926</i>	(3)
FBgn0037643	CG11963	<i>CG11963</i>	(3)
FBgn0039923	CG1793	<i>MED26</i>	(3)
FBgn0053208	CG33208	<i>MICAL</i>	(3)
FBgn0250754	CG42232	<i>CG42232</i>	(3)
FBgn0036622	CG4753	<i>CG4753</i>	(6)
FBgn0031820	CG9537	<i>DLP*</i>	(7)
FBgn0031129	CG1324	<i>CG1324</i>	(8)

*Orthologs of mammalian proteins already reported to bind p53, p63, or p73.

1. Kusch T, Guelman S, Abmayr SM, Workman JL (2003) Two *Drosophila* Ada2 homologues function in different multiprotein complexes. *Mol Cell Biol* 23:3305–3319.
2. Stanyon CA, et al. (2004) A *Drosophila* protein-interaction map centered on cell-cycle regulators. *Genome Biol* 5:R96.
3. Formstecher E, et al. (2005) Protein interaction mapping: A *Drosophila* case study. *Genome Res* 15:376–384.
4. Secombe J, Parkhurst SM (2004) *Drosophila* Topors is a RING finger-containing protein that functions as a ubiquitin-protein isopeptide ligase for the hairy basic helix-loop-helix repressor protein. *J Biol Chem* 279:17126–17133.
5. Bereczki O, et al. (2008) TATA binding protein associated factor 3 (TAF3) interacts with p53 and inhibits its function. *BMC Mol Biol* 9:57.
6. Giot L, et al. (2003) A protein interaction map of *Drosophila melanogaster*. *Science* 302:1727–1736.
7. Bodai L, et al. (2007) Daxx-like protein of *Drosophila* interacts with Dmp53 and affects longevity and Ark mRNA level. *J Biol Chem* 282:36386–36393.
8. *Droid* (V4.0), available at <http://www.droidb.org/>.

Table S3. Enrichment analysis of gene ontology (GO) definitions and phenotypes in the IVDI dataset

GO or phenotype ID	Description	No. of genes	Expected	P value
GO:0007279 (BP)	Pole cell formation	4	0.15	$<10^{-4}$
GO:0007277 (BP)	Pole cell development	4	0.18	$<10^{-4}$
GO:0003704 (MF)	Specific RNA polymerase II transcription factor activity	5	0.53	$<10^{-3}$
GO:0007282 (BP)	Cystoblast division	3	0.15	$<10^{-3}$
GO:0007276 (BP)	Gamete generation	13	4.41	$<10^{-3}$
GO:0019953 (BP)	Sexual reproduction	13	4.54	$<10^{-3}$
GO:0007349 (BP)	Cellularization	5	0.68	$<10^{-3}$
GO:0045143 (BP)	Homologous chromosome segregation	2	0.04	$<10^{-3}$
GO:0000922 (CC)	Spindle pole	3	0.19	$<10^{-3}$
GO:0009994 (BP)	Oocyte differentiation	6	1.14	$<10^{-3}$
FBcv0000366	Female sterile	12	4.08	0.00069
FBcv0000364	Sterile	13	5.43	0.0027
FBcv0000435	Neuroanatomy defective	10	4.26	0.0097
FBcv0000433	Cytokinesis defective	3	0.51	0.014
FBcv0000398	Memory defective	3	0.63	0.024
FBcv0000397	Learning defective	2	0.32	0.040
FBcv0000370	Male sterile	5	2.00	0.049

BP, biological process; CC, cell compartment; MF, molecular function.

Table S4. Manually curated list of human orthologs of Dmp53 interactors identified during the screening

<i>Drosophila</i> gene	Human ortholog(s)*	
	Gene symbol	Definition
	Regulation of transcription and chromatin binding	
HEAT SHOCK FACTOR	HSF1, HSF2, HSF4	Heat-shock transcription factor 1, 2, 4
APTEROUS	LHX2	LIM homeobox 2
TWIN OF EYELESS	PAX6	Paired box 6
ANTI-SILENCING FACTOR 1 CG14514	ASF1A, ASF1B BRD8	ASF1 anti-silencing function 1 homolog A, B Bromodomain containing 8
	Chaperones	
CG7387	DNAJA3	DnaJ (Hsp40) homolog, A3
MRJ	DNAJB6	DnaJ (Hsp40) homolog, B6
CG11035	DNAJC30	DnaJ (Hsp40) homolog, C30
	RNA binding and processing	
YU	AKAP1	A kinase (PRKA) anchor protein 1
CG10333	DDX23	DEAD (Asp-Glu-Ala-Asp) box polypeptide 23
IGF-II MRNA-BINDING PROTEIN	IGF2BP1, IGF2BP2, IGF2BP3	Insulin-like growth factor 2 mRNA binding protein 1, 2, 3
BICOID STABILITY FACTOR GROWL	LRPPRC MTHFSD	Leucine-rich PPR-motif containing Methenyltetrahydrofolate synthetase domain containing
AGO2	EIF2C1, EIF2C2, EIF2C3, EIF2C4	Argonaute 1, 2, 3, 4
AUBERGINE	PIWIL1, PIWIL2, PIWIL3	Piwi-like 1, 2, 3
	Cell cycle	
DOUBLE PARKED	CDT1	Chromatin licensing and DNA replication factor 1
STROMALIN	STAG1, STAG2	Stromal antigen 1, 2
	Centrosomes and cytoskeleton	
ABNORMAL SPINDLE	ASPM	asp (abnormal spindle) homolog, microcephaly associated
CHROMOSOME BOWS	CLASP1	Cytoplasmic linker associated protein 1
SPINDLE ASSEMBLY ABNORMAL 6	SASS6	Spindle assembly 6 homolog
SPAGHETTI SQUASH	MYL9	Myosin, light chain 9, regulatory
TROPOMYOSIN 1	TPM3	Tropomyosin 3
	Enzymatic activity	
FORMALDEHYDE DEHYDROGENASE	ADH5	Alcohol dehydrogenase 5 (class III)
ADENOSYLHOMOCYSTEINASE AT 13	AHCY	S-adenosylhomocysteine hydrolase
CG11652	DPH1	DPH1 homolog, OVCA1
CG10426	INPP5E	Inositol polyphosphate-5-phosphatase, 72 kDa
CG1074	TRMT11	tRNA methyltransferase 11 homolog
CG31108	TLL5	Tubulin tyrosine ligase-like family member 5
	Various	
CG32627	AGBL2, AGBL3	ATP/GTP binding protein-like 2, 3
CG32560	DAB2IP, RASAL2	DAB2 interacting protein, RAS protein activator-like 2
GAS8	GAS8	Growth arrest-specific 8
CG8801	GTPBP4	GTP binding protein 4
JUNCTOPHILIN	JPH1, JPH2, JPH3	Junctophilin 1, 2, 3
CG7139	N4BP2	NEDD4 binding protein 2
MURASHKA	RNF38, RNF44	Ring finger protein 38, 44

Table S4. Cont.

<i>Drosophila</i> gene	Human ortholog(s)*	
	Gene symbol	Definition
CG6686	SART1	Squamous cell carcinoma antigen recognized by T cells
GUSTAVUS	SPSB1, SPSB4	splA/ryanodine receptor domain and SOCS box containing 1, 4
	Unknown	
GRYZUN	C4orf41	
CG13436	C6orf165	
CG8783	C16orf35	
CG9987	C22orf28	
	p53 interologs	
DAXX-LIKE PROTEIN	DAXX	Death-associated protein 6
SIMILAR	HIF1A	Hypoxia-inducible factor 1, alpha subunit
CG7379	ING1,ING2	Inhibitor of growth family, member 1, 2
REPLICATION PROTEIN A 70	RPA1	Replication protein A1, 70 kDa
BAP60	SMARCD1, SMARCD2, SMARCD3	SWI/SNF related, matrix associated, actin-dependent regulator of chromatin, subfamily D, member 1, 2, 3
	Mitochondrial	
CG10932	ACAT1	Acetyl-CoA acetyltransferase
UPSTREAM OF RPII140	C3orf1	
COPROPORPHYRINOGEN OXIDASE	CPOX	Coproporphyrinogen oxidase
CG4769	CYC1	Cytochrome c-1
MITOCH. RIBOSOMAL PROTEIN L16	MRPL16	Mitochondrial ribosomal protein L16
CG8102	NDUFV1	NADH dehydrogenase (ubiquinone) flavoprotein 1
CG8728	PMPCA	Peptidase (mitochondrial processing) alpha
TOM40	TOMM40	Translocase of outer mitochondrial membrane 40 homolog
	Extracellular, intraorganelle, integral to plasma membrane	
NORD	C4orf31	Unknown protein (contains N-terminal signal peptide)
CG31738	FNDC3A	Fibronectin type III domain containing 3A
CG30059	GNS	Glucosamine (N-acetyl)-6-sulfatase (Sanfilippo disease IIID)
CG5919	IDI1	Isopentenyl-diphosphate delta isomerase 1
INFLATED	ITGA8, ITGAV	Integrin alpha 8, alpha V
MMP2	MMP17	Matrix metalloproteinase 17 (membrane-inserted)

Databases: Homologene, version 62, released June 12, 2008; Inparanoid, version 6.0, updated August 2007; TreeFam, version 6.0, released June 6, 2008.

*Orthologs were defined according to Homologene and Inparanoid databases, protein BLAST searches, and phylogenetic tree analysis.